

Spin-orbit coupled Bose-Einstein condensate in a tilted optical lattice

Jonas Larson*

*NORDITA, Se-106 91 Stockholm, Sweden and
Department of Physics, Stockholm University, AlbaNova University Center, SE-106 91 Stockholm, Sweden*

Jani-Petri Martikainen and Anssi Collin
NORDITA, Se-106 91 Stockholm, Sweden

Erik Sjöqvist

*Department of Quantum Chemistry, Uppsala University, Box 518, Se-751 20 Uppsala, Sweden and
Centre for Quantum Technologies, National University of Singapore, 3 Science Drive 2, 117543 Singapore, Singapore*
(Dated: November 14, 2018)

Bloch oscillations appear for a particle in a weakly tilted periodic potential. The intrinsic spin Hall effect is an outcome of a spin-orbit coupling. We demonstrate that both these phenomena can be realized simultaneously in a gas of weakly interacting ultracold atoms exposed to a tilted optical lattice and to a set of spatially dependent light fields inducing an effective spin-orbit coupling. It is found that both the spin Hall as well as the Bloch oscillation effects may coexist, showing, however, a strong correlation between the two. These correlations are manifested as a transverse spin current oscillating in-phase with the Bloch oscillations. On top of the oscillations originating from the periodicity of the model, a trembling motion is found which is believed to be atomic *Zitterbewegung*. It is argued that damping of these *Zitterbewegung* oscillations may to a large extent be prevented in the present setup considering a periodic optical lattice potential.

PACS numbers: 03.75.Mn, 67.85.Hj, 71.70.Ej

I. INTRODUCTION

Recent years have seen an increased interest in many-particle spin dynamics, also termed *spintronics* [1]. Most of this research have been devoted to condensed matter systems, where the electron spin constitutes the spin degree of freedom [2]. However, related or equivalent phenomena may occur by considering the polarization of light [3] or internal Zeeman levels of cold atoms exposed to optical light fields [4] or spatially varying magnetic fields [5].

In many of the spintronics schemes developed in the condensed matter community, a spin-orbit (SO) coupling plays a crucial role for the dynamics. The particular form of the SO coupling can be of either Rashba [6] or Dresselhaus [7] type, both being frequently analyzed in terms of an effective gauge force [8, 9]. In other words, one can interpret the SO couplings as giving rise to an effective spin-dependent Lorentz-type force. Thus, the SO coupling can serve as a spin-filter or a Stern-Gerlach apparatus. As the manufacturing techniques improves, undesired effects deriving from crystal impurities can be greatly suppressed and several successful experiments demonstrating the SO coupling and its outings have been reported recently [10]. Ultracold atoms in optical lattices [11, 12] possess another possibility to implement effective SO couplings, and the study of it within a clean environment. While in condensed matter settings where

the coupling is an intrinsic property of the systems, for cold atoms it has to be externally created via spatially varying laser fields.

Ever since the pioneering experiments on Bose-Einstein condensation (BEC) [13], the field has witnessed a tremendous progress both experimentally and theoretically [14]. The dispersive dipole coupling between light and atoms enables the possibilities to study matter waves in periodic potentials and the experimental realization of model systems discussed within theoretical solid state physics [11]. Today, both the weakly interacting atomic gases as well as more strongly interacting ones can be realized experimentally. Furthermore, utilizing the internal atomic hyperfine levels enable studies of the interplay between internal and external degrees of freedom [15]. One interesting feature is the realization of artificial gauge potentials by means of coupling of internal atomic Zeeman levels [16–19]. The technique of light induced gauge potentials allows for non-Abelian behavior to be analyzed and the SO couplings are one such example [20, 21].

In this paper, we investigate the dynamics of a spinor BEC subjected both to a two-dimensional weakly tilted optical square lattice as well to a set of spatially varying light fields giving rise to an effective SO coupling between the internal atomic states. Thereby, its dynamics will be driven by two mechanisms, namely; (i) Bloch oscillations (BOs) arising due to the tilting of the lattice, and (ii) an intrinsic spin Hall effect (SHE) deriving from the effective SO coupling. The two phenomena may be analyzed in terms of an extrinsic force along the longitudinal direction of the lattice tilt and an intrinsic transverse force. Being orthogonal to each other, these

*Electronic address: jolarson@fysik.su.se

forces render a complex correlated motion of the BEC in the lattice potential. Furthermore, the particular form of the SO coupling renders Dirac cones characterized by linear dispersions reminiscent of relativistic electrons. As an outcome of these, the evolution possesses as well a trembling *Zitterbewegung* motion [22]. Normally, such effect damps out very fast [23], but we show that in a lattice situations as in the present paper it may indeed be long-lived and hence more easily observable. Moreover, the optical lattice can serve as trapping potential for the atoms in the BO regime and no confining Harmonic trap is needed which would typically prevent buildup of spin currents [24].

While SO couplings arise as an intrinsic property in many crystals, in cold atom systems it has to be implemented externally. This, at the one hand may be a source for experimental errors, but at the other it gives a handle for the SO coupling; its strength and form can be tuned experimentally. The same holds for the optical lattice, the lattice strength and geometry are both control parameters, which has made it possible to observe BOs for BECs in optical lattices [25]. Due to the large atomic mass compared to the mass of the electron, *Zitterbewegung* is expectedly more clearly manifested in atomic systems. The first experiments detecting *Zitterbewegung* in atomic systems were recently carried out [23, 26]. A different but related setup can be found in Ref. [5], where a spinor condensate accelerating in a periodic magnetic field was studied. We note that in Ref. [5], the spatially dependent magnetic field gives rise to an effective gauge force. However, Bloch oscillations were not considered, and moreover, in the present work the periodic potential is external and independent of the SO coupling.

The outline of the paper is as follows. In Sec. II, we introduce the model system and outline how effective SO couplings are rendered in such systems. To start with we analyze the free case in which the problem is analytically solvable and demonstrate the SHE and the *Zitterbewegung* effect. Applying the acceleration theorem we also solve the problem under constant acceleration. The dispersions, once an optical lattice has been included, are solved numerically displaying the Dirac cones. Section III presents the main analysis. The full numerical results are presented, where we demonstrate the presence of a SHE and how it is modified by the longitudinal oscillatory motion. In particular, it is shown that the Hall current will also oscillate, however with an increasing oscillation amplitude. On top of the oscillations deriving from the motion in a periodic potential, we find a persisting *Zitterbewegung* effect. Finally, we conclude with a summary in Sec. IV.

II. MODEL SYSTEM

Rashba [6] and Dresselhaus [7] SO couplings appear in a variety of solids, ranging from semiconductors [27], thin magnetic films [28], to graphene [29]. The SO cou-

plings bring about a degeneracy in the energy dispersions. Around these degeneracies, the dispersions are linear, reminiscent to that of relativistic particles, and therefore they are called *Dirac cones*. The relativistic properties have been confirmed experimentally in graphene either by *angle resolved photoemission spectroscopy* or by considering the conductivity and cyclotron motion of electrons [30, 31]. The SO coupling and its corresponding degeneracy induces as well a non-trivial effective gauge structure, giving rise to phenomena such as the intrinsic spin and anomalous Hall effects [8, 9]. In the field of cold atoms, the first light induced effective magnetic fields were demonstrated in Ref. [19], and signatures of non-Abelian structures were recently observed, see [32] and reference therein. BOs with ultracold atoms have already been realized experimentally by numerous groups [25, 33]. We proceed by presenting a scheme which realizes the desired SO coupling in an atomic tripod system.

A. Light induced effective spin-orbit coupling

The idea of effective gauge potentials arising from adiabatic evolution dates back to the seminal works by Mead on vibrations of molecules [34]. Berry [35] generalized this finding by demonstrating the existence of an effective gauge structure in the context a quantum adiabatic evolution. Wilczek and Zee [36] further generalized Berry's result and found an effective non-Abelian gauge potential accompanying adiabatic evolution of degenerate energy eigenstates. Dum and Olshanii [16] showed that the effective gauge potentials can be generated in systems of ultracold atoms subjected to spatially dependent light fields that couple internal atomic states. Following an approach for creating non-Abelian gauge potentials in time-dependent systems [37], Ruseckas *et al.* [17] outlined a scheme how to achieve effective non-Abelian gauge potentials by considering an atomic tripod system in spatially dependent light fields. The coupled four-level system possesses two degenerate dark states that, within certain parameter regimes, can be decoupled from the remaining two bright states via standard adiabatic elimination. The flexibility of this tripod system, deriving from different laser configurations, allows for a variety of phenomena to be studied, such as, e.g., relativistic properties [26, 38, 39], SHEs [40], novel phases of the BEC [41], and topological defects as effective magnetic monopoles [42] or vortices [32].

In the present paper we consider a tripod setup similar to the one described in Refs. [20, 21]. The details of atomic and laser configurations rendering the gauge potentials can be seen in Fig. 1. The internal dynamics, is driven by three lasers that couple the three lower atomic states $|1\rangle$, $|2\rangle$, and $|3\rangle$ to the excited state $|0\rangle$. Parameterizing the laser fields as $\Omega_1 = \Omega \sin \theta \cos \varphi e^{iS_1}$, $\Omega_2 = \Omega \sin \theta \sin \varphi e^{iS_2}$, and $\Omega_3 = \Omega \cos \theta e^{iS_3}$, such that $\Omega = \sqrt{|\Omega_1|^2 + |\Omega_2|^2 + |\Omega_3|^2}$, the two degenerate dark

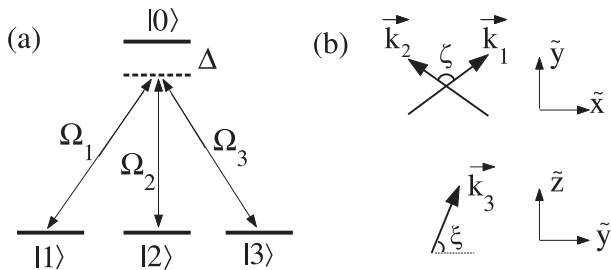


FIG. 1: Atomic (a) and laser (b) configurations. The specific laser arrangement, made up of standing and traveling waves, is described in detail in the text.

states of the corresponding Hamiltonian can be written as

$$\begin{aligned}
 |u_1\rangle &= \frac{1}{\sqrt{2}} \left(\left[e^{-i\pi/4} \cos\theta \cos\varphi + e^{i\pi/4} \sin\varphi \right] e^{-iS_{13}} |1\rangle \right. \\
 &\quad + \left[e^{-i\pi/4} \cos\theta \sin\varphi - e^{i\pi/4} \cos\varphi \right] e^{-iS_{23}} |2\rangle \\
 &\quad \left. - e^{-i\pi/4} \sin\theta |3\rangle \right), \\
 |u_2\rangle &= \frac{1}{\sqrt{2}} \left(\left[e^{-i\pi/4} \cos\theta \cos\varphi - e^{i\pi/4} \sin\varphi \right] e^{-iS_{13}} |1\rangle \right. \\
 &\quad + \left[e^{-i\pi/4} \cos\theta \sin\varphi + e^{i\pi/4} \cos\varphi \right] e^{-iS_{23}} |2\rangle \\
 &\quad \left. - e^{-i\pi/4} \sin\theta |3\rangle \right),
 \end{aligned} \tag{1}$$

where $S_{kl} = S_k - S_l$. Provided the field amplitude Ω is much larger than the atom-light detuning Δ (as depicted in Fig. 1), the two dark states can be safely eliminated from the two bright states, resulting in an effective two-level system [17]. To derive an effective SO coupling between the two internal dark states $|u_1\rangle$ and $|u_2\rangle$, we choose $S_1 = S_2$, $S_{31} = v_s y$, $\varphi = v_\varphi x$, and $\theta \in [0, \pi]$. This can be achieved by coupling the two ground states $|1\rangle$ and $|2\rangle$ to the excited state $|0\rangle$ with two lasers intersecting with an angle ζ and propagating in the xy -plane. These lasers correspond to a standing wave in the x -direction and a plane wave in the y -direction. A third laser, couples the states $|3\rangle$ and $|0\rangle$, and is a plane wave in the yz -plane with an angle ξ of propagation relative to the y -axis. In terms of the angles ζ and ξ , and the wave numbers $k_j = |\vec{k}_j|$, $j = 1, 2, 3$, we have

$$\begin{aligned}
 S_1 &= S_2 = k\tilde{y} \cos(\zeta/2), \\
 S_3 &= k_3\tilde{y} \cos\xi, \\
 \varphi &= 2k\tilde{x} \sin(\zeta/2),
 \end{aligned} \tag{2}$$

with $k \equiv k_1 = k_2$. Performing the adiabatic elimination, taking into account that $\Omega \gg |\Delta|$ and the fact

that we consider ultracold atoms so that excitations due to atomic motion can be neglected, the effective single particle two-level Hamiltonian becomes in dimensionless variables [20]

$$\hat{H}_{\text{eff}}^{(0)} = \hat{p}_x^2 + \hat{p}_y^2 + \hat{p}_z^2 + \delta_0 \hat{\sigma}_z - v_0 \hat{\sigma}_x \hat{p}_x - v_1 \hat{\sigma}_y \hat{p}_y, \tag{3}$$

where δ_0 is an effective Zeeman splitting, $v_0 = (v_\varphi/2) \cos\theta$, $v_1 = (v_s/2) \sin^2\theta/2$. The Pauli matrices $\hat{\sigma}_j$, $j = x, y, z$, operate in the space spanned by the dark states, i.e., $\hat{\sigma}_x = |u_1\rangle\langle u_2| + |u_2\rangle\langle u_1|$, $\hat{\sigma}_y = -i|u_1\rangle\langle u_2| + i|u_2\rangle\langle u_1|$, and $\hat{\sigma}_z = |u_1\rangle\langle u_1| - |u_2\rangle\langle u_2|$. The p -dependence of the last two terms originates from non-adiabatic couplings [43]. We note that these do not include p_z and as a consequence the z -dependence can be fully factored out. In Eq. (3), we have used dimensionless parameters. Explicitly, when we further on introduce a lattice potential whose wave number is k , we let the characteristic length scale be $l = 2\pi k^{-1}$ and we let the characteristic energy scale be the recoil energy $E_R = \hbar^2 k^2 / 2m$. Consequently, time t is measured in units of $\tau = \hbar / E_R$. The superscript (0) indicates the free Hamiltonian in absence of a spatially dependent optical lattice potentials.

The Zeeman shift δ_0 splits the degeneracy of the two internal states and together with the SO coupling it gives rise to a transverse current, an intrinsic anomalous Hall effect. We will, however, focus on the intrinsic SHE obtained when $\delta_0 = 0$. In this case, the transverse particle current vanishes but, on the other hand, a transverse spin current persists. The $\delta_0 = 0$ condition can be achieved by internal Stark shift of the individual bare atomic levels [20, 44]. Thus, in the following we will assume $\delta_0 = 0$, and furthermore we will also consider the symmetric SO coupling characterized by $v_0 = v_1 \equiv v_{so}$. It should be pointed out, however, that even by lifting these constrains an interplay between transverse and longitudinal atomic motion will still occur.

One important prerequisite for successful application of the current scheme is that the system can be prepared in the dark subspace spanned by $\{|u_1\rangle, |u_2\rangle\}$. This issue has been discussed in [45]. The idea is to slowly turn on the external lasers Ω_k , $k = 1, 2, 3$, such that the state follows adiabatically states in the dark subspace, preparing a superposition of $\{|u_1\rangle, |u_2\rangle\}$ but no bright state components.

B. Analytical results without a lattice potential

We note that we may rewrite the Hamiltonian in Eq. (3) ($\delta_0 = 0$) as

$$\hat{H}_{\text{eff}}^{(0)} = (\hat{p}_x - \hat{\mathcal{A}}_x)^2 + (\hat{p}_y - \hat{\mathcal{A}}_y)^2 + \hat{\Phi} \tag{4}$$

with the vector potential

$$(\hat{\mathcal{A}}_x, \hat{\mathcal{A}}_y) = -v_{so} (\hat{\sigma}_x, \hat{\sigma}_y) / 2 \tag{5}$$

and the scalar potential

$$\hat{\Phi} = -\frac{1}{2} v_{so}^2 \hat{1}. \tag{6}$$

These potentials constitute vector and scalar parts of the effective gauge potential. Although being constant in space, the vector potential gives rise to a non-trivial effective gauge field due to its non-Abelian structure, $[\hat{\mathcal{A}}_x, \hat{\mathcal{A}}_y] \neq 0$. Explicitly, this effective field is given by the antisymmetric field tensor

$$\hat{\mathcal{F}}_{kl} = \partial_k \hat{\mathcal{A}}_l - \partial_l \hat{\mathcal{A}}_k - i[\hat{\mathcal{A}}_k, \hat{\mathcal{A}}_l], \quad k, l = x, y, \quad (7)$$

resulting in $\hat{\mathcal{F}}_{xy} = \frac{1}{2}v_{so}^2 \hat{\sigma}_z$ and $\hat{\mathcal{F}}_{kl} = 0$ otherwise. As a result, the spin-orbital motion of the electrons can be understood in terms of an effective Lorentz-type force, akin to that found by Wong [46] for a color-charged classical particle moving in a non-Abelian gauge field. The corresponding force operator may be derived from Heisenberg equations of motion according to [47]

$$\begin{aligned} \hat{\mathbf{F}}_{SO} &= \frac{1}{2} \frac{d^2 \hat{\mathbf{r}}}{dt^2} = \frac{1}{2} [\hat{H}_0, [\hat{\mathbf{r}}, \hat{H}_0]] \\ &= v_{so}^2 (\hat{\mathbf{p}} \times \mathbf{e}_z) \hat{\sigma}_z, \end{aligned} \quad (8)$$

where it is understood that the operators on the right-hand side are all given in the Heisenberg representation and the prefactor $\frac{1}{2}$ in front of the acceleration is the mass in the chosen units. Note that the force in the y -direction is proportional to $-\hat{p}_x$ and the force in the x -direction is proportional to \hat{p}_y . This demonstrates the transverse character of $\hat{\mathbf{F}}_{SO}$ and its equivalence to a Lorentz or Coriolis force. The crucial aspect of Eq. (8) is, however, that the force is state dependent: atoms in dark state $|u_1\rangle$ feel a force with opposite sign compared to those in dark state $|u_2\rangle$. Therefore, the motion of the particles in the xy -plane may separate the two spin states implying that a non-zero spin current is generated. In the following, we shall call the x -direction longitudinal and the y -direction transverse.

The effect of the above Lorentz-type gauge force can be examined by computing how the initial ($t = 0$) state

$$\Psi(p_x, p_y, 0) = \psi_1(p_x, p_y, 0)|u_1\rangle + \psi_2(p_x, p_y, 0)|u_2\rangle \quad (9)$$

evolves in time under influence of $\hat{H}_{\text{eff}}^{(0)}$. We assume that the internal and momentum states of the atom are initially uncorrelated and that the initial momentum states are Gaussian wave packets of the form

$$\begin{aligned} \psi_1(p_x, p_y, 0) &= -\psi_2(p_x, p_y, 0) = \psi(p_x, p_y) \\ &= \frac{1}{\sqrt[4]{4\pi\Delta_p^2}} e^{-\frac{(p_x - p_0)^2 + p_y^2}{2\Delta_p^2}}, \end{aligned} \quad (10)$$

where Δ_p sets the momentum uncertainty and p_0 is the average momentum along the x -direction. This choice corresponds to the pure internal atomic state $|-\rangle = (|u_1\rangle - |u_2\rangle)/\sqrt{2}$. Given this initial state, the time evolved state is readily obtained as

$$\Psi(p_x, p_y, t) = \psi_1(p_x, p_y, t)|u_1\rangle + \psi_2(p_x, p_y, t)|u_2\rangle \quad (11)$$

with

$$\begin{aligned} \psi_1(p_x, p_y, t) &= \frac{1}{\sqrt{2}} [\cos(\lambda t) + i \sin(\lambda t) e^{-i\theta}] \\ &\quad \times \psi(p_x, p_y) e^{-i(p_x^2 + p_y^2)t}, \\ \psi_2(p_x, p_y, t) &= -\frac{1}{\sqrt{2}} [\cos(\lambda t) + i \sin(\lambda t) e^{i\theta}] \\ &\quad \times \psi(p_x, p_y) e^{-i(p_x^2 + p_y^2)t}. \end{aligned} \quad (12)$$

Here, we have used the energy dispersions E_{\pm} and the energy eigenstates ϕ_{\pm} of the Hamiltonian in Eq. (3), which read

$$\begin{aligned} E_{\pm}(p_x, p_y) &= p_x^2 + p_y^2 \pm \lambda, \\ |\phi_{\pm}\rangle &= \frac{1}{\sqrt{2}} (\pm |\uparrow\rangle + e^{i\theta} |\downarrow\rangle), \end{aligned} \quad (13)$$

where $\lambda = v_{so} \sqrt{p_x^2 + p_y^2}$ and $\tan(\theta) = p_y/p_x$.

In Fig. 2 we display the dimensionless averages

$$\langle \hat{y} \rangle_i = 2i \iint \psi_i^*(p_x, p_y, t) \frac{\partial}{\partial p_y} \psi_i(p_x, p_y, t) dp_x dp_y, \quad (14)$$

with $i = 1, 2$. The factor 2 derives from normalization of the individual wave packet components. Since the initial velocity is along the longitudinal x -direction, the deviation from $\langle \hat{y} \rangle_i = 0$ is a direct consequence of the state-dependent Lorentz-type gauge force $\hat{\mathbf{F}}_{SO}$. Note that $\langle \hat{y} \rangle_1 = -\langle \hat{y} \rangle_2$ giving a vanishing transverse particle current. This symmetry is broken by keeping the Zeeman term $\delta_0 \hat{\sigma}_z$ in the Hamiltonian of Eq. (3). The particle current induced by such a $\hat{\sigma}_z$ -term goes under the name intrinsic anomalous Hall effect. After $t \approx 20$, the separation of the two internal dark states has reached an asymptotic value. Until $t \approx 20$, the transverse spin current shows an oscillating behavior deriving from the same mechanism as the one underlying relativistic Zitterbewegung in the Dirac equation [22]. In the Dirac equation the trembling motion describes coherent coupling between positive and negative energy solutions, while in the present situation it describes population swapping between the internal states. In solids, the amplitude of these oscillations become extremely small due to the lightness of the electron, while in atomic or ionic systems the heavier masses imply larger amplitudes and possible detection [23, 26]. Despite heavier masses, the rapid damping of the trembling motion as depicted in Fig. 1 is a limitation also in atomic/ionic Zitterbewegung experiments [23, 26]. In the next subsection we will argue how this decay may be prevented by studying the effect in the presence of an optical lattice.

In order to generate a current in the system one applies a constant longitudinal force $F_{ex} \mathbf{e}_x$, e.g., induced by gravitation in atomic systems. In the particular case of solids, the force derives from a voltage across the solid, and the electrons reach a steady state motion in which the applied force is balanced by scattering against crystal

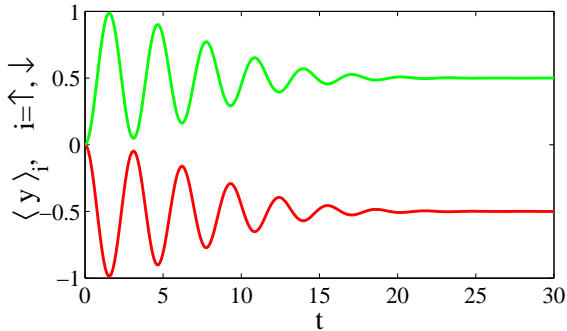


FIG. 2: (Color online) Time evolution of $\langle \hat{y} \rangle_{1,2}$ (green curve correspond to the dark state $|u_1\rangle$ and the red curve correspond to the dark state $|u_2\rangle$) as defined in Eq. (14). The dimensionless parameters in Eqs. (3) and (10) are $v_{so} = 1$ ($= v_1 = v_2$), $\delta_0 = 0$, $p_0 = 1$, and $\Delta_p = 0.1$. The initial state is thus a Gaussian with a non-zero average momentum along the x -direction.

impurities. On the other hand, a system of cold atoms is, to a good approximation, free from impurities and one would therefore achieve constant acceleration. Assuming that the force is weak and that the total time of evolution is relatively short, we can perform an adiabatic approximation, consisting in replacing p_x by $p_x - F_{ex}t$ in Eq. (12). Hence, the momentum grows linearly in time in accordance with classical motion. How this comes about can be easily understood by considering the time evolution of the Hamiltonian $\hat{H} = \hat{H}_0 - F_{ex}\hat{x}$ for small forces F_{ex} and times t . In this regime, the time-evolution operator can be approximated accordingly

$$\hat{U}(t) = e^{-i\hat{H}t} \approx e^{iF_{ex}\hat{x}t} e^{-i\hat{H}_0 t}, \quad (15)$$

so that the first exponential gives the coupled time-evolution while the second simply boosts the x -momentum by $-F_{ex}t$. For longer time periods, the large velocity rendered by the acceleration will typically cause non-adiabatic excitations, which we neglect for the moment. Similarly, for large values of $F_{ex}t$, the factorization of the exponentials is no longer justified. The resulting averages $\langle \hat{y} \rangle_i$ calculated within this approximation are depicted in Fig. 3. As before, we encounter a build-up of a transverse spin current but in this case the current changes sign after some time and finally there is no net spin separation. By comparison with a full numerical integration of the Hamiltonian we find that the imposed adiabatic approximation breaks down after relatively short times. Nevertheless, numerically we have verified that the dynamics beyond this approximation goes as well asymptotically to zero for large times. We believe that the origin of this result is a complicated interplay between the transverse and longitudinal forces, together

with the coupling between the two internal states. For spinless particles, the two forces render a spirally transverse motion and hence a net transverse current. For particles with spin-dependent Lorentz forces $\hat{\mathbf{F}}_{SO}$ one would expect a net transverse spin current, but the coupled nature of the two spin states seems to destroy such spin current in the case of constant acceleration.

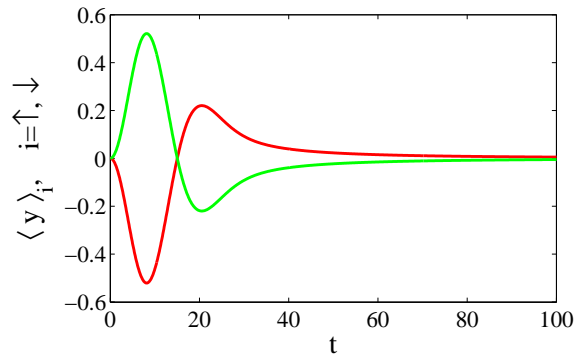


FIG. 3: (Color online) Same as Fig. 2, but with a constant weak force of magnitude F_{ex} in the x -direction added to the Hamiltonian (3) and assuming the validity of the adiabatic approximation. The dimensionless parameters are $v_{so} = 1$, $\delta_0 = 0$, $p_0 = 0$, $\Delta_p = 0.1$, and $F_{ex} = 0.01$.

C. Band spectrum and the acceleration theorem

In the following section we numerically investigate the dynamics in the presence of an optical lattice. Insight into the evolution behavior is gained by considering the spectrum of the Hamiltonian including a lattice potential while disregarding the linear force potential. Adding to the SO Hamiltonian in Eq. (3) a spatially oscillating periodic potential, yields

$$\hat{H} = \hat{p}_x^2 + \hat{p}_y^2 + v_{so}(\hat{p}_x\hat{\sigma}_x + \hat{p}_y\hat{\sigma}_y) + V \cos^2(\hat{x}) + V \cos^2(\hat{y}). \quad (16)$$

The Hamiltonian is periodic and consequently possesses a band-gap spectrum $E_\nu(k_x, k_y)$ with associated Bloch eigenstates $u_{\nu, k_x, k_y}(x, y)$, characterized by a discrete band-index $\nu = 1, 2, 3, \dots$ and quasi-momentum numbers (k_x, k_y) restricted to the first Brillouin zone, i.e., $-1 \leq k_x < 1$ and $-1 \leq k_y < 1$. A detailed study of Bloch theory in the presence of SO couplings can be found in Ref. [48]. The first two bands $E_1(k_x, k_y)$ and $E_2(k_x, k_y)$, obtained from numerical diagonalization of the Hamiltonian, are shown in Fig. 4. A similar band structure has been obtained in Ref. [39] for cold atoms in a square optical lattice. We directly see the effect of the SO coupling in terms of Dirac cones at $(k_x, k_y) = (n, m)$, where

$n, m = -1, 0, 1$. It is further seen that the ground state is not the $u_{1,0,0}(x, y)$ Bloch state, as for a regular square lattice lacking SO couplings. This fact is at the heart of the *Jahn-Teller effect* [49], where the Dirac cone (or *conical intersection* as it is usually referred to when it appears in position space rather than in momentum space) induces a symmetry breaking that lowers the ground state energy. Furthermore, we note that the two lowest bands are not gapped, while there is a gap between the second and third band. Indeed, due to the SO coupled two-level structure of the Hamiltonian, the bands come in pairs where each pair possesses Dirac cones for quasi-momenta $(k_x, k_y) = (n, m)$. The effective number of Dirac cones is four (easily seen by shifting the Brillouin zone by $\frac{1}{2}$ in both directions), compared to two Dirac cones encountered in honeycomb lattices, like in graphene. We notice that recently it was shown how more complex lattice potentials may render single Dirac cones within the first Brillouin zone [50].

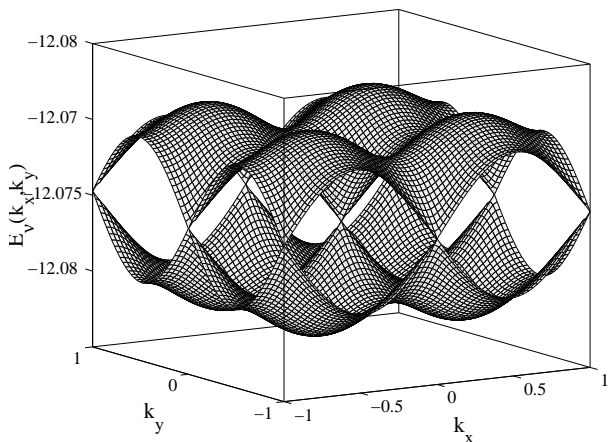


FIG. 4: The two lowest Bloch bands $E_\nu(k_x, k_y)$ for a square lattice with Rashba spin-orbit coupling. In this example, $v_{so} = 1$ and $V = 5$.

In the adiabatic regime, a non-zero extrinsic force $F_{ex}\mathbf{e}_x$ is treated by using the same approximation as above, yielding

$$u_{\nu, k_x, k_y}(x, y) \rightarrow u_{\nu, k_x - F_{ex}t, k_y}(x, y). \quad (17)$$

In the presence of a periodic potential, this adiabatic assumption has become known as the *acceleration theorem* [51]. It implies that no population is transferred between the individual bands ν . As a direct consequence, an initial state with well localized quasi-momentum within one single band will show an oscillatory motion rather than a constantly accelerating one, once the extrinsic force $F_{ex}\mathbf{e}_x$ has been turned on. These are the well studied Bloch oscillations [52], which have

been experimentally verified in a variety of systems, such as cold atomic gases [33], BECs [25], semiconductor superlattices [53], waveguide arrays [54], and photonic crystals [55].

BOs are clearly an outcome of the periodic potential and its characteristic energy spectrum possessing gaps of forbidden energies at the center and edges of the Brillouin zone. As the amplitude of the potential V vanishes, the gaps close and the acceleration theorem breaks down. In particular, for weak lattice amplitudes, the gap between the first two energy bands scales as $\sim V$. By linearizing the dispersions around the band gap and replacing k_x by $k_x - F_{ex}t$, one obtains a realization of the celebrated *Landau-Zener model* [56]. Here, k_x is the initial quasi-momentum in the x -direction. This model is analytically solvable, giving the probability of population transfer between the two states of the corresponding bands. It has been shown that the decay of BOs can be correctly estimated using the Landau-Zener theory [25, 57].

In the present model, the situation becomes qualitatively different. At the Dirac points, the gap vanishes and the acceleration theorem cannot be imposed. However, from Fig. 4 it is seen that the Dirac cones appear between the first two bands, and not between the second and third band. Hence, assuming a state initially prepared on the lowest band one may expect predominant population transfer between the $\nu = 1$ and $\nu = 2$ bands and not to higher bands. Thereby, further acceleration is hindered by the gap between the second and third band and spin-dependent BOs may still be encountered. In other words, a modified acceleration theorem involving pair of bands could result. In fact, as already mentioned, the acceleration theorem is a specific example of the more general adiabatic theorem, and in molecular and chemical physics it has long been known that adiabaticity breaks down in the vicinity of a conical intersection [58]. In this context, it should be kept in mind that adiabaticity is a widespread concept in physics, and the general definition concerns systems whose dynamics is governed by an explicitly time-dependent Hamiltonian. Adiabaticity, as it appears in the acceleration theorem, is in this sense more reminiscent of the *Born-Oppenheimer approximation* [58], applicable to time-independent Hamiltonians describing light and heavy quantal degrees of freedom corresponding here to the spin and the spatial motion, respectively, of the particles.

III. NUMERICAL RESULTS

Our numerical analysis will be restricted to a system consisting of weakly interacting atoms, for which a mean-field description is expected to capture the phenomena we are interested in. In the s -wave scattering regime, we thereby consider dynamics rendered by a spinor Gross-Pitaevskii equation [14, 21]

$$\begin{aligned}
i\frac{\partial}{\partial t}\Psi(x, y, t) = & \left\{ -\left(\frac{\partial^2}{\partial x^2} + \frac{\partial^2}{\partial y^2}\right) + V(\cos^2(x) + \cos^2(y)) - F_{ex}x + v_{so} \begin{bmatrix} 0 & -i\frac{\partial}{\partial x} - \frac{\partial}{\partial y} \\ -i\frac{\partial}{\partial x} + \frac{\partial}{\partial y} & 0 \end{bmatrix} \right. \\
& \left. + \begin{bmatrix} g_{11}n_1(x, y, t) + g_{12}n_2(x, y, t) & 0 \\ 0 & g_{12}n_1(x, y, t) + g_{22}n_2(x, y, t) \end{bmatrix} \right\} \Psi(x, y, t).
\end{aligned} \tag{18}$$

Here,

$$\Psi(x, y, t) = \begin{bmatrix} \langle x, y | u_1 | \Psi(t) \rangle \\ \langle x, y | u_2 | \Psi(t) \rangle \end{bmatrix} = \begin{bmatrix} \psi_1(x, y, t) \\ \psi_2(x, y, t) \end{bmatrix} \tag{19}$$

is a two-component spinor wave function of the dark states, $n_i(x, y, t) = |\psi_i(x, y, t)|^2$, F_{ex} the external longitudinal force, and g_{11} , g_{22} and g_{12} are the effective s -wave scattering amplitudes related to the scattering lengths a_i as $g_i = N4\pi\hbar^2 a_i / (3E_R\sqrt{2\pi}l_z m)$, where l_z is the width of the single site wave function in the z -direction. This definition of g_i implies that the wave function has been normalized as $\int |\Psi(x, y, t)|^2 dx dy = 1$. In the basis of dark states, the scattering lengths are effective ones different from the regular hyperfine scattering lengths. Nevertheless, the ratio between the two scattering amplitudes should approximately be the same regardless of basis, and, in particular, for a spinor condensate such as that of ^{87}Rb one has $g_{11} \approx g_{22} \approx g_{12}$ [59]. We will restrict the analysis to repulsive interactions, $g_{12}, g_{22}, g_{12} > 0$, and we will furthermore assume $g_{11} = g_{22} = g_{12} \equiv g$ [59].

In the absence of a lattice, the SO coupling gives rise to a non-Abelian Mead-Berry curvature [34–36], which results in a transverse splitting of spin components, the intrinsic SHE. However, in Figs. 2 and 3 the motion along the longitudinal x -direction was either constant or monotonously accelerating, while for a weakly tilted lattice, where BOs dominate the longitudinal motion, it is neither clear how the transverse spin current nor how the trembling Zitterbewegung motion will be manifested. For instance, will there be sufficient time for a transverse spin current to be established within a single Bloch period? In Ref. [60], the intrinsic anomalous Hall effect was studied in a single particle system confined by an harmonic potential and hence the motion was as well oscillatory as in the case of BOs. The transverse current appeared as a rotation on top of the harmonic oscillatory motion, i.e., in polar coordinates (r, φ) the gauge potential causes a non-zero current in the φ -direction. Such current would indeed be zero for an SO coupling possessing an Abelian structure rather than non-Abelian, e.g. for couplings on the form $v_{so}(\hat{\sigma}_\alpha \hat{p}_x + \hat{\sigma}_\alpha \hat{p}_y)$ with $\alpha = x, y, z$. It is clear that a corresponding rotational current cannot be strictly encountered in the present system since exact polar symmetry is broken by the tilting of the lattice and by the lattice in itself.

The time evolution of the system is solved by employing the split-operator approach [61]. The method relies

on factorizing the time-evolution operator into a spatial part and a momentum part valid in the limit of infinitely small time-step propagation. One convenient feature of this method is that the wave function is in principle obtained at any instant of time in both position $\Psi(x, y, t)$ and momentum $\tilde{\Psi}(p_x, p_y, t)$ space. Furthermore, for a system bounded from below, the approach is capable of giving an approximate ground state of the system by simply propagating it sufficiently long in imaginary time.

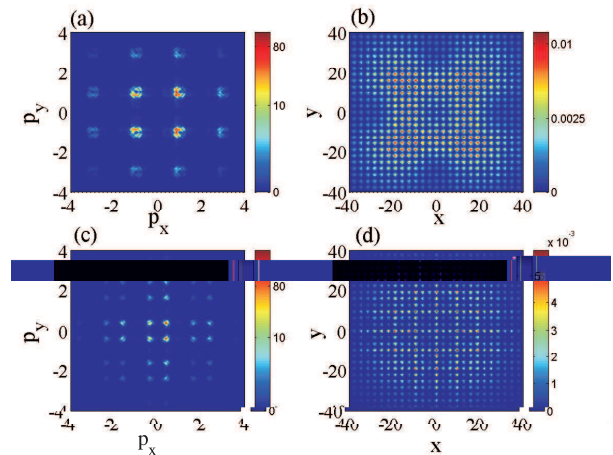


FIG. 5: (Color online) Absolute value of the ground state wave function in momentum space (a) and (c), and in position space (b) and (d). The dimensionless parameters are $V = 5$, $F_{ex} = 0$, and $g = 1$ for all plots, $v_{so} = 2$ in the upper plots (a) and (b), and $v_{so} = 1$ in the lower plots (c) and (d). Thus, the lower plots correspond to the dispersions depicted in Fig. 4.

Our numerical considerations will focus on propagation of an initial (approximated) ground state for the untilted ($F_{ex} = 0$) lattice. That is, we consider the ground state of a spin-orbit coupled BEC in an optical lattice, and then we introduce a quantum quench by suddenly switch on a linear force in the x -direction. Hence, we begin by propagating an ansatz function in imaginary time with zero extrinsic force $F_{ex} = 0$. When convergence of the imaginary time evolution has been reached, we switch to real time propagation, including the extrinsic force by adding the potential term $-F_{ex}\hat{x}$ to the Hamiltonian. As predicted by the acceleration theorem, for short times the weak forces F_{ex} will induce a linear increase in the quasi-momentum k_x . In contrast to BOs in a regular square

lattice, here the SO coupling implies that also the quasi-momentum k_y is indirectly affected by the force F_{ex} . At the same time, the build up of motion in the y -direction induces an intrinsic force F_{SO} along the longitudinal x -direction of BOs. In addition, the linear dispersions induce a trembling Zitterbewegung motion. It is thereby likely to expect a complex motion arising from the interplay between the two forces related to SHE and BOs and the outcomes from linear dispersions.

Figure 5 displays the absolute values of the initial ground state wave function achieved via imaginary time evolution for $F_{ex} = 0$. The momentum wave functions depicted in (a) and (c) demonstrate the Jahn-Teller effect as the ground state populates non-zero momentum states [49]. The lower two plots (c) and (d) correspond to the parameters of the two lowest Bloch bands shown in Fig. 4. The fact that the ground state obtained from this numerical method is not symmetric, as seen from the plots, is believed to have a two-fold cause. First, it seems to derive from the fact that the imaginary time evolution is taken only up to a point where the state evolution has approximately converged, and, secondly, from the fact that even small fluctuations can result in an asymmetric ground state, due the four-fold degeneracy of the ground state of our Hamiltonian. In fact, the complete convergence of the ground state has not been reached since the position space wave functions depicted in (b) and (d) are localized in contradiction to the true ground state having a Bloch structure, and furthermore since the momentum wave functions have a finite width. This, however, should not be seen as a shortcoming since normally one would cool the atomic gas in the presence of a confining potential which would result in a localized gas. In addition, if the propagated state extends over the full lattice one would run into troubles when quantities such as the mean spatial position is calculated numerically. Note that the momentum wave functions of (a) and (c) are different from the quasi-momentum as is evident in the multiple Bragg components separated by $\Delta p_x, \Delta p_y = \pm 1$. In other words, even though the momentum wave functions extend beyond the first Brillouin zone, it populates, to a very good approximation, only the lowest band. We also note that the position space ground state wave functions, shown in (b) and (d), predominantly populate the individual lattice sites. Hence, only judging from Figs. 5 (b) and (d) it would be difficult to predict the presence of a SO coupling and the Dirac cones that derive from it, which instead manifest themselves in momentum space in terms of a Jahn-Teller effect.

In order to analyze the interplay between the transverse and longitudinal forces, \mathbf{F}_{SO} and $F_{ex}\mathbf{e}_x$, we calcu-

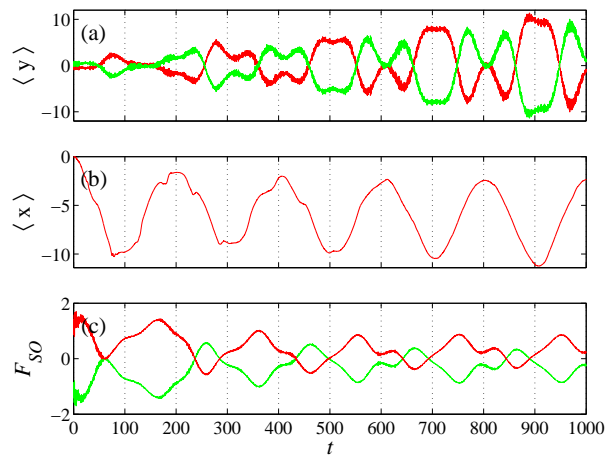


FIG. 6: (Color online) Average transverse position $\langle \hat{y} \rangle$ (a), average longitudinal position $\langle \hat{x} \rangle$ (b), and average intrinsic force F_{SO} in the transverse direction (c). Red lines correspond to the dark state $|u_1\rangle$ while green lines to $|u_2\rangle$. For $\langle \hat{x} \rangle$ the two lines are identical because of symmetry reasons. The dimensionless parameters are the same as in Fig. 5 (a) and (b), but now with a non-zero extrinsic force, $F_{ex} = 0.01$.

late

$$\begin{aligned} \langle \hat{y} \rangle_i &= \frac{1}{N_i} \int |\psi_i(x, y, t)|^2 y dx dy, \\ \langle \hat{x} \rangle_i &= \frac{1}{N_i} \int |\psi_i(x, y, t)|^2 x dx dy, \\ \langle F_{SO}^{(y)} \rangle_i &= -g_{so}^2 \frac{1}{N_i} \int |\tilde{\psi}_i(p_x, p_y, t)|^2 p_x dp_x dp_y, \end{aligned} \quad (20)$$

with $i = 1, 2$ corresponding to averages in terms of the two dark states $|u_1\rangle$ and $|u_2\rangle$, respectively, $N_j = \iint |\psi_j(x, y, t)|^2 dx dy$, and the last quantity is the intrinsic force in the y -direction. We find that $\langle \hat{x} \rangle_1 = \langle \hat{x} \rangle_2$ (up to numerical accuracy) and therefore plot only one of the two components.

Our numerical results are presented in Figs. 6 and 7. The difference between the two figures lies in the scattering amplitude g . In Fig. 7 the effective scattering amplitude g is already as large as 10 recoil energies E_R and we can thereby conclude that the spin current is rather insensitive to the value of g . It is generally known that strong non-linearity can qualitatively change system properties. In BECs it leads to phenomena such as soliton and vortex creation. Normally the greatest impact of the non-linearity is seen around curve crossings [62]. Beyond a critical value of the non-linearity (in our case $g > g_{crit}$), in one dimension swallowtail loops are formed in the vicinity of the curve crossings characterizing additional stationary non-linear states, e.g. solitons. Up to this critical value the dynamics seems rather insensitive at least on a mean-field level. However, formation of these loops beyond the critical value implies break-

down of the acceleration theorem [63]. To date, it seems that analysis of these effects have been restricted to one dimensional situations and it is therefore not fully understood how non-linearity affects the structure of the Dirac cones appearing in two dimensions. Nonetheless, we have numerically found that the general structure of Figs. 6 and 7 drastically change for very large values of g . All present BO experiments, however, are performed in the weakly interacting regime where it is known that loops are absent, and we thereby restrict our analysis to these experimentally more relevant parameter ranges.

We see from both Fig. 6 and 7 that the x and y motions are indeed correlated; when the Bloch oscillation reaches its turning points, the spin separation in the y -direction is roughly maximal and as the velocity in the longitudinal x -direction changes sign, the spin separation decreases due to the reversed sign of the intrinsic force. When the longitudinal velocity is the greatest (equivalent to maxima of the intrinsic force F_{SO}), the spin current is reversed. More precisely, as the atoms begin to accelerate in the tilted lattice the quasi-momentum k_x increases linearly in time and a spin current is built up in the transverse direction. However, after half a Bloch period the quasi-momentum reaches the Brillouin boundary and the x -motion is stopped and then reversed. Consequently, also the spin current is reversed and one encounters a decreasing spin current in the y -direction. Finally, the spin current has dropped to zero and builds up in the opposite direction instead. Hence, the spin current follows the same oscillatory behavior as the BOs.

One may argue that a large spin separation should be hindered by the alternating sign of the velocity in the x -direction. Nonetheless, from our numerical results depicted in Figs. 6 and 7, we note that the spin separation in the y -direction is relatively large. Indeed, $\langle \hat{y} \rangle$ exceeds several site-spacings and furthermore this separation amplitude increases in time. The fact that neither the oscillatory spin nor the oscillatory longitudinal current show a clean perfect harmonic pattern derives from, at the one hand possible non-adiabatic effects and the breakdown of the acceleration theorem, and at the other that the transverse current induces an intrinsic force $F_{SO}^{(x)}$ in the longitudinal direction which adds to the extrinsic force $F_{ex}\mathbf{e}_x$. The full coupled dynamics is therefore rather complex, but nonetheless, our figures make clear the overall in-phase oscillations between the two currents.

On top of the oscillations of $\langle \hat{x} \rangle_i$, there is a slight drift toward negative values of x . This is an outcome of non-adiabaticity and breakdown of the acceleration theorem. However, this drift is rather small and the dynamics is therefore predominantly adiabatic. This drift can be suppressed by increasing the lattice amplitude V on the cost that the amplitude of longitudinal oscillations decreases. It would not, however, imply a diminishing SHE since it is related to the longitudinal momentum and not position.

A closer look at the two figures reveals that in the transverse motions there is an additional oscillating mo-

tion different from the spin current being in phase with the BOs. This is believed to be Zitterbewegung clearly seen in the freely evolving wavepackets of Fig. 2. Contrary to that figure, here these oscillations do not collapse suggesting that it might be preferable to detect the Zitterbewegung effect within a tilted lattice, compared to the case of freely propagating atoms. The survival of Zitterbewegung should as well derive from the alternating motion due to the optical lattice.

Figures 6 and 7 have been calculated for an approximated initial ground state of the untilted lattice. As already pointed out, experimentally the condensate might be prepared in the presence of an external trap, and then the optical lattice as well as the coupling of the internal states are turned on in such a way that the condensate is not in a true ground state of the coupled system. To analyze the effect of such excitations, we have redone the simulations of Figs. 6 and 7 for an initial Gaussian momentum state of a form depicted in Eq. (10) with $p_0 = 0$ and $\Delta_p = 0.1$. The results are very similar to the ones of Figs. 6 and 7, and we therefore do not present them here. We have also investigated the effect of a shallow harmonic potential in the transverse direction during the evolution in the tilted lattice. Again, a transverse spin current is obtained, however this time the amplitude of transverse oscillations is decreased due to the confining potential. This reduction of spin separation would indeed be present in any experiment utilizing a confining trapping potential. The idea of employing an optical lattice potential as a trapping potential circumvent such shorting. In order to achieve trapping in this case one must stay within the BO regime, i.e. adiabatic. As Figs. 6 and 7 demonstrates, even though the atoms oscillate a relatively large spin current can build up during time.

In relation to the measurability of the spin separation, we may note that even though $|\langle \hat{y} \rangle_1 - \langle \hat{y} \rangle_2|$ is considerably larger than the lattice spacing, it does not imply that the two wave functions $\psi_1(x, y, t)$ and $\psi_2(x, y, t)$ do not spatially overlap. In fact, the overlap is relatively large and fluorescent measurement of a single experimental run would therefore not contain sufficient information to reveal the spin current. However, this is hardly never the case in true experimental realizations and instead an ensemble of measurements should be considered, where the ensemble average gives $|\langle \hat{y} \rangle_1 - \langle \hat{y} \rangle_2|$. Since this value is presumably larger than the lattice spacing, it should indeed be measurable [64]. In the cold atom community, time-of-flight measurements are often employed, in which it is the atomic momentum density that is being measured. If the separation of the momentum wave functions is non-zero, the position space wave functions $\psi_1(x, y, t)$ and $\psi_2(x, y, t)$ will set apart further during the time-of-flight. If this separation is faster than the intrinsic wave function broadening, a finite time-of-flight measurement may enhance the detection efficiency.

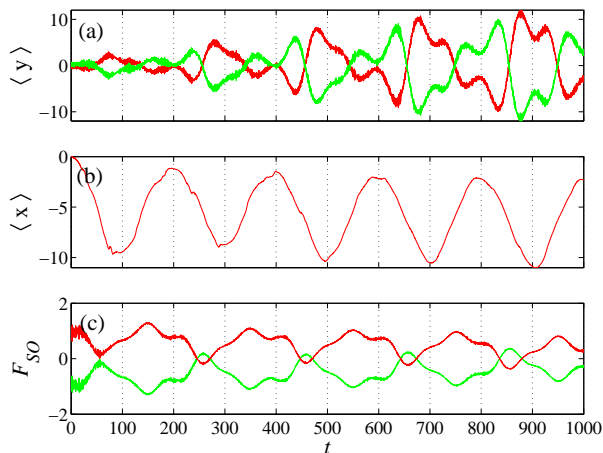


FIG. 7: (Color online) Same as in Fig. 6, but with an increased atom-atom interaction; $g = 10$.

IV. CONCLUSION

In this paper, we have considered an ultracold atomic system possessing three well-studied properties of condensed matter theory, Bloch oscillations, intrinsic spin Hall currents, and Zitterbewegung. Our motivation for this study comes from the fact that Bloch oscillations have been verified in the same type of setups [25, 33], light induced gauge potentials have been demonstrated [18, 19, 32], and Zitterbewegung have been detected in ion-trap experiments [23].

The spin-Hall effect (SHE) and the Bloch oscillations (BO) in our system are driven by two perpendicular forces: the extrinsic force appearing due to tilting of the lattice potential and the intrinsic force originating from the effective gauge potential caused by the spin-orbit (SO) coupling. We demonstrated that the interplay between these two forces gives rise to a correlated motion in the xy -plane, and despite the fact that the BOs are expected to prevent a build up of large transverse spin currents, we argued that the SHE should indeed be detectable. We utilized system parameters that should be achievable in current experiments, e.g., the amplitude of the lattice potential is five recoil energies compared to

the experimentally utilized ones of Ref. [25] ranging from one to 14 recoil energies, and the SO coupling two recoil energies compared to 8 recoil energies in Ref. [19]. For a potential amplitude as large as $14E_r$, the dispersions are almost flat and longitudinal motion is almost frozen. The momentum along the longitudinal direction do, however, oscillate within the Brillouin size and, interestingly and somewhat surprisingly, one would therefore see an oscillating transverse spin Hall current despite lack of longitudinal currents. We furthermore showed that the effects are insensitive to experimentally relevant atom-atom interaction strengths. Entering a strongly interacting gas seemed to affect our results and we argue that this is likely to derive from a non-linearity induced breakdown of adiabaticity around the Dirac points. An additional interesting aspect being discussed is the analogue of relativistic Zitterbewegung. Our numerical results indicate that it may be preferable to consider an optical lattice configuration when studying this effect since it persists over longer time periods. The optical lattice convey as well the possibility to avoid confining trapping potentials preventing large spin currents.

We should also point out that the system presented in this paper allows for many extensions and different phenomena to be studied. For example, vortex generation in lattices [32, 65], Bose-Einstein condensation into non-zero momentum states [66], topologically ordered states of matter [67], or more strongly correlated systems, by means of second quantization of the mean-field Hamiltonian, may find realization in atoms possessing an internal tripod structure and trapped in optical lattices. The flexibility permits as well for various extensions, for example time-dependent lattices or SO couplings. A recent paper considered Zitterbewegung of ultracold atoms for a driven SO coupling [68]. The same idea can be utilized in order to increase the transverse spin current in our model.

Acknowledgments

JL acknowledges support from the MEC program (FIS2005-04627). JL and ES acknowledge financial support from the Swedish Research Council.

[1] I. Zutic, J. Fabian, and S. Das Sarma, *Rev. Mod. Phys.* **76**, 323 (2004).
 [2] S. A. Wolf, D. D. Awschalom, R. A. Buhrman, J. M. Daughton, S. von Molnar, M. L. Roukes, A. Y. Chtchelkanova, and D. M. Treger, *Science* **294**, 1488 (2001).
 [3] M. Onoda, S. Murakami, and N. Nagaosa, *Phys. Rev. Lett.* **93**, 083901 (2004); K. Yu. Bliokh and Yu. P. Bliokh, *Phys. Rev. E* **70**, 026605 (2004); K. Yu. Bliokh and Yu. P. Bliokh, *Phys. Lett. A* **333**, 181 (2004); K. Yu. Bliokh and

Yu. P. Bliokh, *Nat. Photonics* **2**, 748 (2008). O. Hosten and P. G. Kwiat, *Science* **319**, 787 (2008).
 [4] A. M. Dudarev, R. B. Diener, I. Carusotto, and Q. Niu, *Phys. Rev. Lett.* **92**, 153005 (2004); X.-J. Liu, X. Liu, L. C. Kwek, and C. H. Oh, *Phys. Rev. Lett.* **98**, 026602 (2007); J. Y. Vaishnav, J. Ruseckas, C. W. Clark, and G. Juzelunas, *Phys. Rev. Lett.* **101**, 265302 (2008); X.-J. Liu, M. F. Borunda, X. Liu, and J. Sinova, *Phys. Rev. Lett.* **102**, 046402 (2009).
 [5] M. Taillefumier, E. K. Dahl, A. Brataas, and W. Hofstet-

- ter, Phys. Rev. A **80**, 020407(R) (2009).
- [6] Y. A. Bychkov and E. I. Rashba, J. Phys. C. **17**, 6039 (1984).
- [7] G. Dresselhaus, Phys. Rev. **100**, 580 (1955).
- [8] J. Sinova, D. Culcer, Q. Niu, N. A. Sinitsyn, T. Jungwirth, and A. H. MacDonald, Phys. Rev. Lett. **92**, 126603 (2004).
- [9] T. Jungwirth, Q. Niu, and A. H. MacDonald, Phys. Rev. Lett. **88**, 207208 (2002).
- [10] N. Nagaosa, J. Sinova, S. Onoda, A. H. MacDonald, and N. P. Ong, Rev. Mod. Phys. **82**, 1539 (2010); Y. Tian, L. Ye, and X. Jin, Phys. Rev. Lett. **103**, 087206 (2009).
- [11] M. Lewenstein, A. Sanpera, V. Ahufinger, B. Damski, A. Sen, and U. Sen, Adv. Phys. **56**, 243 (2007).
- [12] I. Bloch, J. Dalibard, and W. Zwerger, Rev. Mod. Phys. **80**, 885 (2008).
- [13] M. H. Anderson, J. R. Enscher, M. R. Matthews, C. E. Wieman, and E. A. Cornell, Science **269**, 198 (1995); K. B. Davies, M. O. Mewes, M. R. Andrews, N. J. VanDruten, D. S. Durfee, D. M. Kurn, and W. Ketterle, Phys. Rev. Lett. **75**, 3969 (1995).
- [14] C. J. Pethick and H. Smith, *Bose-Einstein Condensation in Dilute Gases*, (Cambridge University Press, Cambridge, 2008).
- [15] C. J. Myatt, E. A. Burt, R. W. Ghrist, E. A. Cornell, and C. E. Wieman, Phys. Rev. Lett. **78**, 586 (1997); J. Stenger, S. Inouye, D. M. Stamper-Kurn, H.-J. Miesner, A. P. Chikkatur, and W. Ketterle, Nature **396**, 345 (1998); D. M. Stamper-Kurn, H. J. Miesner, A. P. Chikkatur, S. Inouye, J. Stenger, and W. Ketterle, Phys. Rev. Lett. **83**, 661 (1999); O. Mandel, M. Greiner, A. Widera, T. Rom, T. W. Hänsch, and I. Bloch, Phys. Rev. Lett. **91**, 010407 (2003); L. E. Sadler, J. M. Higbie, S. R. Leslie, M. Vengalattore, and M. S. Stamper-Kurn, Nature **443**, 312 (2006); J. Larson and J.-P. Martikainen, Phys. Rev. A **80**, 033605 (2009).
- [16] R. Dum and M. Olshanii, Phys. Rev. Lett. **76**, 1788 (1996).
- [17] J. Ruseckas, G. Juzeliunas, P. Öhberg, and M. Fleischhauer, Phys. Rev. Lett. **95**, 010404 (2005).
- [18] S. K. Dutta, B. K. Teo, and G. Raithel, Phys. Rev. Lett. **83**, 1934 (1999).
- [19] Y.-J. Lin, R. L. Compton, A. R. Perry, W. D. Phillips, J. V. Porto, and I. B. Spielman, Phys. Rev. Lett. **102**, 130401 (2009); Y.-J. Lin, R. L. Compton, K. Jiménez-García, J. V. Porto, and I. B. Spielman, Nature **462**, 628 (2009).
- [20] T. D. Stanescu, C. Zhang, and V. Galitsky, Phys. Rev. Lett. **99**, 110403 (2007).
- [21] J. Larson and E. Sjöqvist, Phys. Rev. A **79**, 043627 (2009).
- [22] B. Thaller, *The Dirac Equation*, (Springer Verlag, Berlin, 1992).
- [23] R. Gerritsma, G. Kirchmair, F. Zahringer, E. Solano, R. Blatt, and C. F. Roos, Nature **463**, 68 (2010).
- [24] It is worth pointing out that even if a confining trap is absent in the actual BO experiments, it is present during the condensation process and as it is turned off before releasing the condensate in the tilted lattice it implies, in the local density approximation, that the chemical potential varies within the extent of the atomic cloud which renders a source for decoherence, see [25].
- [25] O. Morsch, J. H. Müller, M. Cristiani, D. Ciampini, and E. Arimondo, Phys. Rev. Lett. **87**, 140402 (2001); M. Cristiani, O. Morsch, J. H. Müller, D. Ciampini, E. Arimondo, Phys. Rev. A **65**, 063612 (2002); J. H. Denschlag, J. E. Simsarian, H. Häffner, C. McKenzie, A. Browaeys, D. Cho, K. Helmerson, S. L. Rolston, and W. D. Phillips, J. Phys. B: At. Mol. Opt. Phys. **35**, 3095 (2002); M. Gustavsson, E. Haller, M. J. Mark, J. G. Danzl, G. Rojas-Kopeinig, and H.-C. Nägerl, Phys. Rev. Lett. **100**, 080404 (2008).
- [26] J. Y. Vaishnav and C. W. Clark, Phys. Rev. Lett. **100**, 153002 (2008).
- [27] F. Miralles and G. Kirczenow, Phys. Rev. B **64**, 024426 (2001); L. W. Molenkamp, G. Schmidt, and G. E. W. Bauer, Phys. Rev. B **64**, 121202 (2001).
- [28] A. Kasic, M. Schubert, S. Einfeldt, D. Hommel, and T. E. Tiwald, Phys. Rev. B **62**, 7365 (2000).
- [29] T. Ando, J. Phys. Soc. Japan **69**, 1757 (2000); C. L. Kane and E. J. Male, Phys. Rev. Lett. **95**, 226801 (2005); H. Min, J. E. Hill, N. A. Sinitsyn, B. R. Sahu, L. Kleinman, and A. H. MacDonald, Phys. Rev. B **74**, 165310 (2006).
- [30] S. Y. Zhou, G.-H. Gweon, J. Graf, A. F. Federov, C. D. Spataru, R. D. Diehl, Y. Kopelevich, D.-H. Lee, S. G. Louie, and A. Lanzara, Nature Phys. **2**, 595 (2006).
- [31] K. S. Novoselov, A. K. Geim, S. V. Morozov, D. Jiang, M. I. Katsnelson, I. V. Grigorieva, S. V. Dubonos, and A. A. Firsov, Nature **438**, 197 (2005).
- [32] T.-L. Ho and S. Zhang, arXiv:1007.0650.
- [33] M. BenDahan, E. Peik, J. Reichel, Y. Castin, and C. Salomon, Phys. Rev. Lett. **76**, 4508 (1996).
- [34] C. A. Mead and D. G. Truhlar, J. Chem. Phys. **70**, 2284 (1979); C. A. Mead, Chem. Phys. **49**, 23 (1980); C. A. Mead, Chem. Phys. **49**, 33 (1980); C. A. Mead, Rev. Mod. Phys. **64**, 51 (1992).
- [35] M. V. Berry, Proc. R. Soc. London Ser. A **392**, 45 (1984).
- [36] F. Wilczek and A. Zee, Phys. Rev. Lett. **52**, 2111 (1984).
- [37] R. G. Unanyan, B. W. Shore, and K. Bergmann, Phys. Rev. A **59**, 2910 (1998).
- [38] G. Juzeliunas, J. Ruseckas, A. Jacob, L. Santos, and P. Öhberg, Phys. Rev. Lett. **100**, 200405 (2008).
- [39] J.-M. Hou, W.-X. Yang, and X.-J. Liu, Phys. Rev. A **79**, 043621 (2009).
- [40] S.-L. Zhu, H. Fu, C.-J. Wu, S.-C. Zhang, and L.-M. Duan, Phys. Rev. Lett. **97**, 240401 (2006).
- [41] T. D. Stanescu, B. Anderson, and V. Galitsky, Phys. Rev. A **78**, 023616 (2008).
- [42] V. Pietilä and M. Möttönen, Phys. Rev. Lett. **102**, 080403 (2009).
- [43] J. Larson and S. Stenholm, Phys. Rev. A **73**, 033805 (2006).
- [44] A. Jacob, P. Öhberg, G. Juzeliunas, and L. Santos, Appl. Phys. B **89**, 439 (2007).
- [45] G. Juzeliunas, J. Ruseckas, M. Lindberg, L. Santos, and P. Öhberg, Phys. Rev. A **77**, 011802(R) (2008).
- [46] S. K. Wong, Nouvo Cimento **65** A, 689 (1970).
- [47] B. K. Nikolic, L. P. Zarbo, and S. Welack, Phys. Rev. B **72**, 075335 (2005).
- [48] V. Y. Demikhovskii and D. V. Khmisky, J. Exp. Theo. Phys. **83**, 340 (2006); S. Smirnov, D. Bercioux, and M. Grifoni, Europhys. Lett. **80**, 27003 (2007); D. V. Khmisky, Phys. Rev. B **79**, 205401 (2009).
- [49] H. C. Longuet-Higgins, U. Opik, M. H. L. Pryce, and R. A. Sack, Proc. R. Soc. A **244**, 1 (1958); D. R. Yarkony, Rev. Mod. Phys. **68**, 985 (1996).

- [50] R. Shen, L. B. Shao, B. Wang, and D. Y. Xian, Phys. Rev. B **81**, 041410(R) (2010).
- [51] V. Grecchi and A. Sacchetti, Phys. Rev. B **63**, 212303 (2001).
- [52] F. Bloch, Z. Phys. **52**, 555 (1928); D. I. Choi and Q. Niu, Phys. Rev. Lett. **82**, 2022 (1999).
- [53] K. Leo, P. H. Bolivar, F. Bruggemann, R. Schwedler, and K. Kohler, Solid. Stat. Commun. **84**, 943 (1992); J. Feldmann, K. Leo, J. Shah, D. A. B. Miller, J. E. Cunningham, T. Meier, G. Vonplessen, A. Schulze, P. Thomas, and S. Schmittrink, Phys. Rev. B **46**, 7252 (1992).
- [54] R. Morandotti, U. Peschel, J. S. Aitchison, H. S. Eisenberg, and K. Silberberg, Phys. Rev. Lett. **83**, 4756 (1999); T. Pertsch, P. Dannberg, W. Elflein, A. Brauer, and F. Lederer, Phys. Rev. Lett. **83**, 4752 (1999).
- [55] H. Trompeter, W. Krolikowski, D. N. Neshev, A. S. Desyatnikov, A. A. Sukhorukov, Y. S. Kivshar, T. Pertsch, U. Peschel, and F. Lederer, Phys. Rev. Lett. **96**, 053903 (2006).
- [56] L. D. Landau, Phys. Z. USSR **2**, 46 (1932); C. Zener, Proc. R. Soc. London A **137**, 696 (1932).
- [57] M. Holthaus, J. Phys. B: Quant. Semiclass. Opt. **2**, 589 (2000).
- [58] M. Baer, *Beyond Born-Oppenheimer*, (Wiley, New York, 2006).
- [59] D. S. Hall, M. R. Matthews, J. R. Ensher, C. E. Wieman, and E. A. Cornell, Phys. Rev. Lett. **81**, 4531 (1998).
- [60] J. Larson, Phys. Rev. A **81**, 051803(R) (2010).
- [61] M. D. Flei, J. A. Fleck, and A. Steiger, J. Comp. Phys. **47**, 412 (1982).
- [62] B. Wu and Q. Niu, Phys. Rev. A **61**, 023402 (2000); J. Liu, B. Wu, and Q. Niu, Phys. Rev. Lett. **90**, 170404 (2003); M. Machholm, C. J. Pethick, and H. Smith, Phys. Rev. A **67**, 053613 (2003).
- [63] J. Lie, L. Fu, B.-Y. Ou, S.-G. Chen, D.-I. Choi, B. Wu, and Q. Niu, Phys. Rev. A **66**, 023404 (2002).
- [64] T. Gericke, P. Würtz, D. Reitz, T. Langen, and H. Ott, Nature Physics **4**, 949 (2008); N. Gemelke, X. Zhang, Ch.-L. Hung, and Ch. Chin, Nature **460**, 995 (2009); W. S. Bakr, J. I. Gillen, A. Peng, S. Fölling, and M. Greiner, Nature **462**, 74 (2009); J. F. Sherson, C. Weitenberg, M. Endres, M. Cheneau, I. Bloch, and S. Kuhr, Nature **18**, August (2010).
- [65] K. J. Gunter, M. Cheneau, T. Yefsah, S. P. Rath, and J. Dalibard, Phys. Rev. A **79**, 011604 (2009).
- [66] W. V. Liu and C. Wu, Phys. Rev. A **74**, 013607 (2006).
- [67] T. D. Stanescu, V. Galitski, J. Y. Vaishnav, C. W. Clark, and S. D. Sarma, Phys. Rev. A **79**, 053639 (2009).
- [68] Q. Zhang, J. Gong, and C. H. Oh, Phys. Rev. A **81**, 023608 (2010).